Journal of Theoretical and Applied Vibration and Acoustics 10 (2) 34-49 (2024)

I S A V

Journal of Theoretical and Applied Vibration and Acoustics

journal homepage: http://tava.isav.ir

Design and experimental evaluation of road excitation simulator actuated by electro-hydraulic system

Mohammad Javad Azizi [a], Mehdi Mirzaei [b,*], Sadra Rafatnia [c], Taha Falahati Nodeh [d]

[a] *M.Sc., Faculty of Mechanical Engineering, Sahand University of Technology, Tabriz, 513351996, IRAN*

[b] *Professor, Faculty of Mechanical Engineering,Sahand University of Technology, Tabriz, 513351996, IRAN*

[c] *Assistant Professor, Faculty of Mechanical Engineering, Sahand University of Technology, Tabriz, 513351996, IRAN*

[d] *Ph.D., Faculty of Mechanical Engineering, Sahand University of Technology, Tabriz, IRAN*

Research Article

ARTICLE INFO

Article history:
Received 16 May 2024

Received in revised form
23 November 2024

Accepted 4 January 2024

Available online 11 February 2025

Keywords:
Road excitation simulator

Electro-hydraulic actuator

Time-varying irregularities

Fuzzy controller

Vibration testing

ABSTRACT

This study focuses on the design and experimental evaluation of a road excitation simulator driven by an electro-hydraulic system. The simulator is employed to create road irregularities, which are then applied to the vehicle platform during laboratory testing. To generate the desired road inputs by the simulator, a fuzzy tracking control law is developed based on expert knowledge of the system derived from displacement data obtained from a linear potentiometer transformer. The fuzzy controller utilizes the Mamdani structure to compute the required voltage for the electro-hydraulic directional valves. This controller is implemented through the LabView interface, and its performance is evaluated and compared against a proportional-integral-derivative (PID) controller under various road inputs. Experimental results from tests conducted on a fabricated platform in the laboratory demonstrate that the fuzzy method offers superior accuracy and reliability compared to the PID controller. The designed simulator is capable of generating a variety of standard road inputs for testing the vibrations of various vehicles and their cargo.

* Corresponding author.
E-mail address: mirzaei@sut.ac.ir (M. Mirzaei)

http://dx.doi.org/10.22064/tava.2024.2029276.1240

1. Introduction

The increasing demands of customers, combined with the competitive environment among car manufacturers, have led to significant advancements in modern suspension systems, including passive [1], semi-active [2], and active [3] types. In the context of active suspension systems, advanced optimization algorithms and control strategies are employed to optimize the performance of the suspension in real-time [4, 5]. These systems can respond instantaneously to changes in road conditions and vehicle dynamics, improving safety and driving experience [6, 7]. The primary function of suspension systems is to adjust suspension parameters to enhance ride comfort and vehicle handling across diverse road conditions. The designed suspension systems must undergo laboratory testing under various simulated road irregularities to achieve these goals more effectively.

Developing a standard road profile is essential for vehicle suspension systems, as it serves as the foundation for analyzing system behavior, identifying key parameters, and evaluating the performance of the designed system [8, 9]. In this context, road simulators for suspension systems are commonly designed using electric motors [10, 11], pneumatic actuators [12], electric actuators [13, 14], and hydraulic actuators [15, 16]. Lin et al. [11] incorporated a mesh rotating disc to simulate the road profile. This structure demonstrated the capability to generate road inputs through two bumps. Salmani et al. [10] demonstrated the capability to generate sinusoidal road inputs with constant amplitude and a specific frequency spectrum using an electric motor. Similarly, Akbari and Lohman [14] employed a custom electric actuator to produce road inputs. In these studies, only simple road inputs were generated, bypassing the need to design a controller to achieve the desired road profile.

A literature review reveals various strategies for the position control of electro-hydraulic actuators. For instance, Gue et al. [17] presented a sliding mode controller based on an extended state observer. Similarly, Chen et al. [18] developed a sliding mode controller with adaptive boundary layers for an electro-hydraulic servo system. A nonlinear controller, combined with a high-gain observer, was designed for an electro-hydraulic system [19]. Generally, the efficiency of the model-based control strategies discussed above depends on accurate system modeling. Additionally, applying the full-order model of the electrohydraulic system with high nonlinearities increases the system's order, complicating controller design. Moreover, employing additional sensors to monitor all system states is not financially efficient. Model-free control methods, such as PID controllers [20-22] and fuzzy controllers [23, 24], offer alternative solutions for the position control of electro-hydraulic systems. For example, Wonohadidjojo et al. [23] presented a fuzzy controller for an electro-hydraulic actuator, while Chen et al. [24] utilized an integrated fuzzy controller to achieve synchronous positioning in a dual-cylinder electro-hydraulic system under unbalanced load conditions.

This study focuses on designing a road excitation simulator and the experimental implementation of a Mamdani-based fuzzy logic controller to create road profiles with varying frequencies and amplitudes. A shaft and guide bushing are used to generate vertical motion in the mechanical design of the road profile simulator driven by an electro-hydraulic actuator. A spring with suitable stiffness is included to counterbalance the platform's weight and minimize excessive power consumption in the hydraulic system. A linear potentiometer transformer (LPT) is installed and calibrated in the fabricated setup to measure the platform's displacement.

A fuzzy controller produces a suitable voltage for the electro-hydraulic valve to generate road profiles with different frequencies and amplitudes.

The results from the proposed approach are compared with those from other control strategies to demonstrate its effectiveness in controlling the electro-hydraulic actuator and generating various road profiles.

The main contribution of this work can be summarized as follows:

A novel test platform is designed and fabricated to generate time-varying road irregularities.

An electro-hydraulic actuator is experimentally implemented in a road excitation simulator.

A fuzzy controller is developed based on expert knowledge of the system.

Results are compared with a conventional PID across various reference trajectories.

The structure of the paper is as follows: section 2 gives an overview of the road simulator system. Section 3 outlines the kinetic model of the road profile simulator. In section 4, the fuzzy controller algorithm is developed, and the PID controller, as a conventional method, is introduced. Section 5 discusses the results of the practical implementation. The paper concludes with a summary in the final section.

2. Overall structure of the road simulator platform

Figure 1 illustrates the structure of the proposed control system. The road profile simulator is controlled using an electro-hydraulic actuator. The displacement measurement is facilitated by an LPT sensor mounted on the platform. Communication between the platform and the computer is established using a PCI NI-DAQ-6052 card, which transmits sensor data to the computer and sends control inputs to the digital valve amplifier (DVA) card. LabView software handles data acquisition, processing, and control signal computation. These control signals are transmitted to the DVA card via serial communication. The DVA then converts the digital inputs into precise analog commands, directing a servo valve to control the flow of hydraulic fluid accurately. This enables the electro-hydraulic actuator to convert the hydraulic signals into mechanical motion, ensuring precise positioning of the components.

A shaft and guide bush produce vertical displacement within the road input stimulation system in the mechanical design. Also, a spring with a fixed stiffness has been used to balance the weight of the device and minimize the hydraulic system's power consumption. Therefore, the power consumption in moving up and down is almost equal. On the other hand, to compensate for the partial horizontal movement of the tire in the displacement of the suspension, a sliding plate is used, and the tire is placed on this plate. The schematic design of the road simulation is shown in Figure 2.

It should be noted that the conventional use of electric motors in road profile simulators is generally limited to generating simple sinusoidal road inputs, restricting their capability to replicate more complex or varied road profiles. In contrast, the proposed method, equipped with an electro-hydraulic actuator controlled by a Mamdani-based fuzzy logic controller, enables the simulation of diverse road inputs with varying amplitudes and frequencies. This flexibility allows the system to generate complex and realistic road profiles, providing a more comprehensive platform for testing suspension systems under a wide range of conditions.

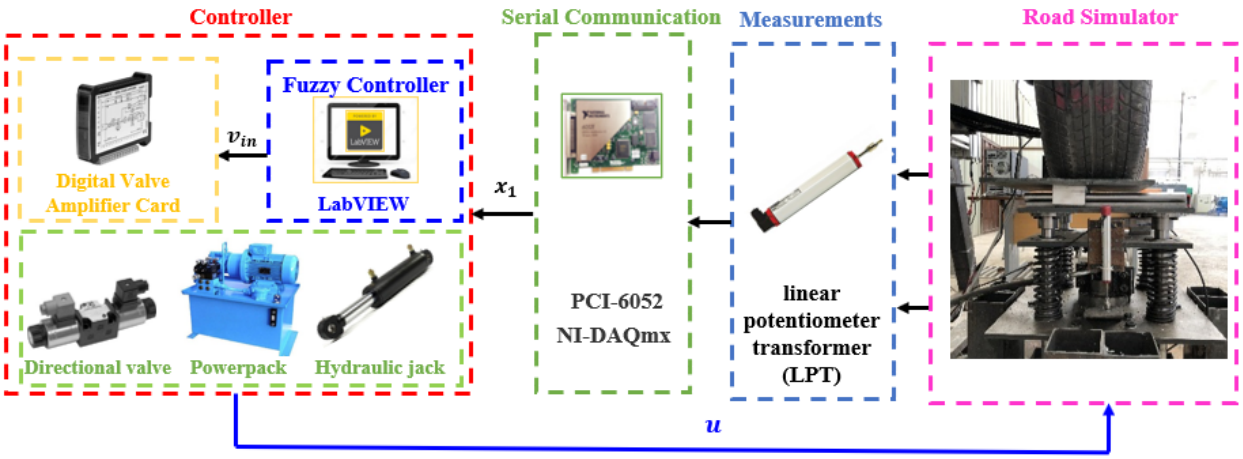

Figure 1. The overview of the proposed system

.

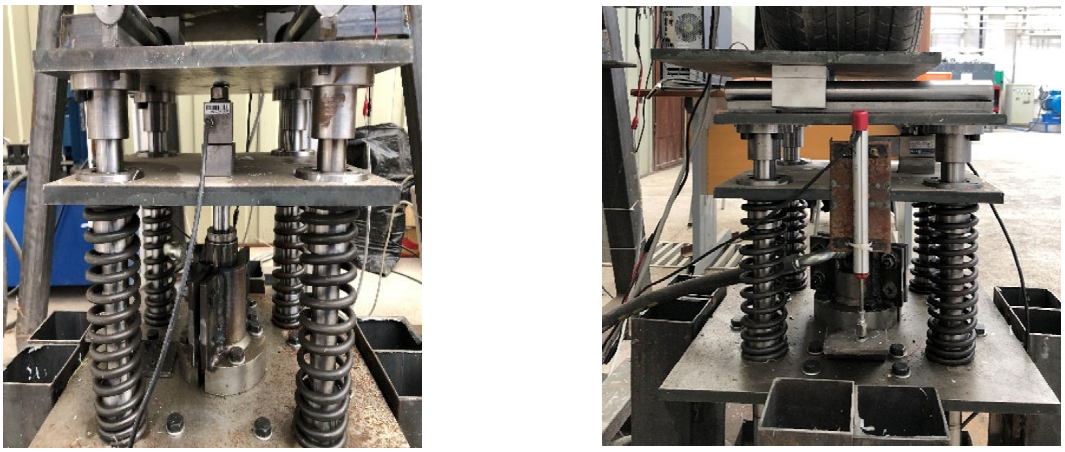

(a) (b)

Figure 2. Schematic of the simulator, (a) Front view, (b) Side view

An electro-hydraulic actuator is utilized to generate the control force in the system. The main components of the hydraulic actuator and its power system are depicted in Figure 3. As shown in this figure, the power pack of the hydraulic system comprises a Duplomatic proportional directional valve and a Duplomatic proportional pressure control valve that regulates the oil flow to the hydraulic jack. Other components of the hydraulic system are numbered in Figure 3 and presented in Table 1.

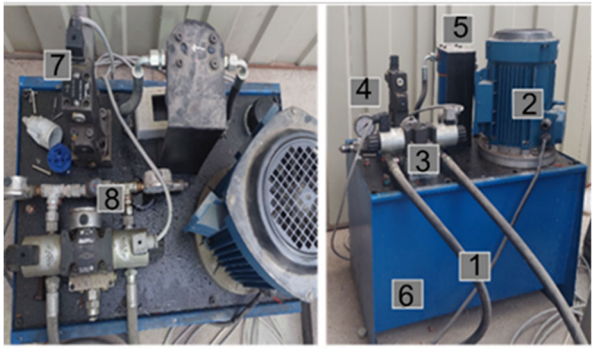

Figure 3. Hydraulic actuator components.

Table 1. Components of hydraulic actuator power pack

1-Hydraulic hose	2-Hydraulic pump	3-Flow control valve
4-Pressure manometer	5-Oil filter	6-Oil tank
7-Pressure control valve	8-Pressure control key	

3. Dynamic model of mechanism

Figure 4 presents a schematic of the platform, which incorporates an electro-hydraulic actuator along with a set of springs. According to Figure 6 and assuming a linear behavior for the spring assembly, the governing equations in the state-space form are derived as follows:

$$\dot{x}_1 = x_2 \tag{1}$$

$$\dot{x}_2 = \frac{K_r}{m_b} x_1 - \frac{u}{m_b} \tag{2}$$

in which x_1 and x_2 represent the system's vertical displacement and velocity, respectively. Additionally, K_r denotes the spring coefficient of the structure and m_b is the total mass of the platform, and u is the control input. The parameters of the system are presented in Table 2. Note that the proposed system is specifically designed for vehicular suspension testing, and the parameters specified in Table 2 are based on the quarter-car weight in a realistic suspension system. Additionally, the spring parameter is selected to compensate for the device's weight and to prevent increased power consumption of the hydraulic system.

Table 2. Parameters of the system

#Par.	#Value
m_b#	349 kg#
k_r#	#190000N/m

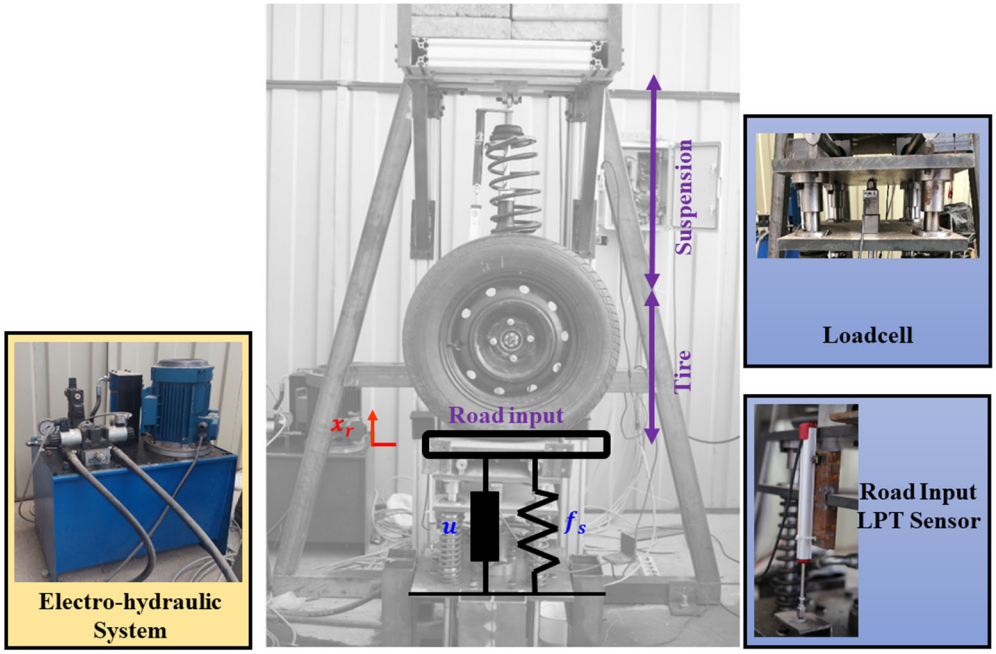

Figure 4. The road simulator structure.

This study utilizes an electro-hydraulic actuator to generate the control force. As shown in Figure 5, the actuator contains a servo spool valve, which is activated by voltage. The movement of the spool valve directs high-pressure fluid to either the upper or lower chamber of the cylinder, while the opposite side is connected to the oil tank. This fluid flow generates a pressure differential across both sides of the piston. Consequently, the active force produced by the actuator is the result of the pressure difference multiplied by the piston area.

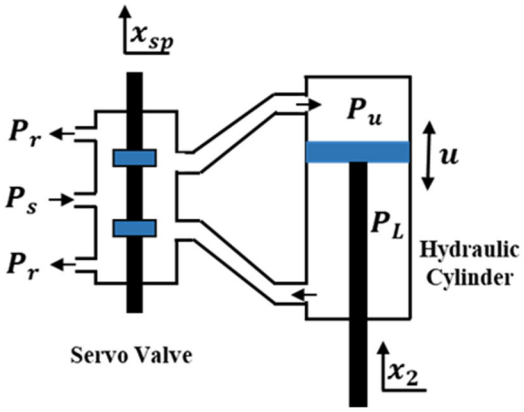

Figure 5. schematic of the electro-hydraulic valve.

#

The dynamics of the hydraulic actuator can be presented as follows [25, 26]:

$$u = AP_L \tag{3}$$

$$\frac{v_t}{4\beta}\dot{P}_L = Q_L - C_t P_L - A\mathrm{x}_2 \tag{4}$$

$$Q_L = C_d \omega x_v \mathrm{sgn}(P_s - P_L \mathrm{sgn}(x_v)) \sqrt{\frac{1}{p}|P_s - P_L \mathrm{sgn}(x_v)|} \tag{5}$$

where, u represents the force extracted by the hydraulic actuator, P_L denotes the pressure difference across the piston, A denotes the cross-sectional area of the piston, v_t is the total volume of the actuator cylinder, β is the effective bulk modulus, Q_L and C_t indicate the hydraulic flow rate and the total leakage modulus of the piston, respectively. Additionally, C_d is the discharge modulus, and ω is the slope of the spool valve. The displacement of the hydraulic valve is shown as xv, ρ is the density of the hydraulic fluid, and P_s denotes the pressure generated by the hydraulic pump. By defining these parameters as

$$\alpha = \frac{4\beta}{\mathrm{v_t}}, \quad \beta = \alpha \mathrm{C_t}, \quad \gamma = \alpha \mathrm{C_t} \omega \sqrt{\frac{1}{\rho}} \tag{6}$$

and the integration of equations (4) and (6) leads to

$$\dot{\mathrm{P}}_\mathrm{L} = -\beta \mathrm{P_L} - \alpha \mathrm{A x_2} + \gamma \mathrm{x_v} \mathrm{sgn}(\mathrm{P_s} - \mathrm{P_L} \mathrm{sgn}(\mathrm{x_v})) \sqrt{|\mathrm{P_s} - \mathrm{P_L} \mathrm{sgn}(\mathrm{x_v})|} \tag{7}$$

Additionally, the displacement of the hydraulic valve spool, considering the time delay τ, is related to the input voltage v_{in} as follows:

$$\dot{\mathrm{x}}_\mathrm{v} = \frac{1}{\tau}(-\mathrm{x_v} + \mathrm{v_{in}}) \tag{8}$$

4. Control system design

The main aim of the controller is to reduce the tracking error between the output excitation profile and the desired one. In this structure, the voltage of the proportional directional valve is considered as the control input. At the same time, the displacement of the platform, measured by an LPT, is defined as the system output. In the following, two different control methods are investigated to provide the reference road profile.

4.1. Fuzzy controller

The electro-hydraulic actuator is a complex nonlinear system that includes different sources of uncertainties. In this paper, a fuzzy controller is implemented to provide an efficient real-time controller for the proposed mechanism. The structure of the proposed controller is shown in Figure 6. The tracking error, $e(t)$ and its variation $\Delta e(t)$ is used as the input of the controller, and the voltage of the servo valve is determined as the controller's output.

Note that the difference between an instance tracking error and the delayed one is used as a variation of the tracking error in the LabView software.

The proposed method combines the principles of fuzzy logic with the structure of a proportional-derivative (PD) controller. Unlike traditional PD controllers, which rely on precise mathematical models, fuzzy PD controllers are adept at managing systems with nonlinearities, uncertainties, or complex dynamics. The proposed controller converts the error and its variation into linguistic variables represented by fuzzy sets. These linguistic variables are then used to formulate a rule, relating the inputs to the controller output. Through fuzzification, inference, and defuzzification, the controller computes a crisp control signal that guides the system toward the desired setpoint. Note that Kc in the output of the fuzzy system is the gain value for converting the output of the fuzzy system to the voltage of the electro-hydraulic valves.

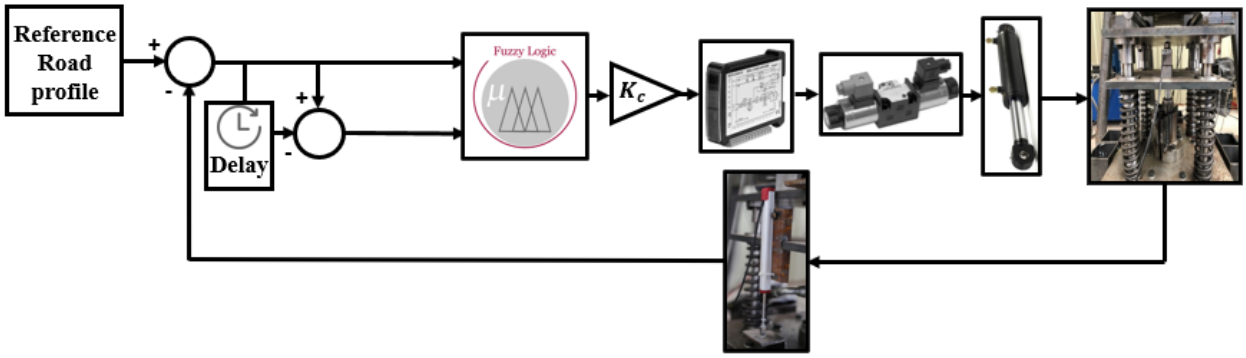

Figure 6. Fuzzy control system structure

The membership functions for the fuzzy system's input and output variables are depicted in Figure 7. These membership functions are developed with careful consideration to capture the nuanced behavior of the tracking error $e(t)$ and its variation $\Delta e(t)$, effectively. The linguistic variables associated with $e(t)$ and $\Delta e(t)$ are defined as "NB" (Negative Big), "NS" (Negative Small), "ZE" (Zero), "PS" (Positive Small), and "PB" (Positive Big). For the output control variable u, these linguistic terms correspond to proportional responses that effectively counterbalance the tracking error, ensuring the system's stability and rapid response. The design of the membership functions and fuzzy rules draws on a knowledge-based approach. In this setup, the boundaries of each membership function were determined with guidance from domain experts. The fuzzy control consists of 25 rules, structured in Table 3, to handle various combinations of tracking error and its rate of change. These rules are based on principles of control theory and expert recommendations, ensuring that the system behaves intuitively in response to different error scenarios. For example:

When both $e(t)$ and $\Delta e(t)$ are significantly positive, a large negative control output is required to counteract the error and bring it back toward zero.

Conversely, if $e(t)$ and $\Delta e(t)$ are both strongly negative, the system increases the control input positively, pushing the system state back toward equilibrium.

In this structure, each rule can be represented as follows:

If $e(t)$ is A and $\Delta e(t)$ is B, then u is C (9)

where A, B, and C are fuzzy sets that are defined based on input and output domains. The defuzzification process is handled through the center of area (CoA) method, a widely used approach in fuzzy systems due to its balanced representation of the control output. By calculating the centroid of the area under the aggregated output curve, the CoA method provides a smooth and interpretable control input, essential for achieving stable control in dynamic environments. This method effectively translates the qualitative insights from fuzzy inputs into a precise, actionable control output.

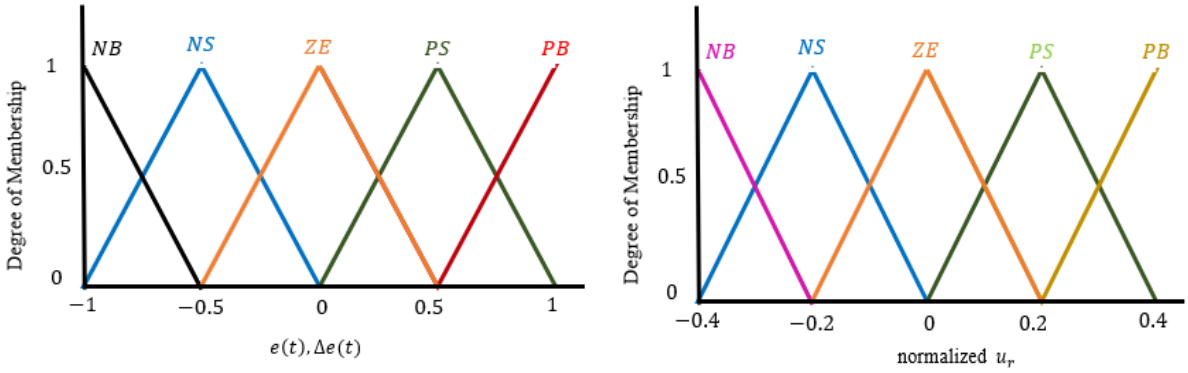

(a) (b)

Figure 7. Fuzzy logic membership functions, (a) Inputs, (b) Outputs.

Table 3. Introduction of membership functions

$e(t), \Delta e(t)$#	**NB**	**NS**	**Z**	**PS**	**PB**
NB	PB	PB	PB	PS	ZE
NS	PB	PB	PS	ZE	NS
ZE	PB	PS	ZE	NS	NB
PS	PS	ZE	NS	NB	NB
PB	ZE	NS	NB	NB	NB

4.2. PID controller

The PID controller is a commonly employed feedback control system for managing electro-hydraulic actuators [15, 16, 27]. PID control is a closed-loop method combining three control modes: proportional, integral, and derivative. The proportional control creates a control without drastic changes. The integral control corrects system errors, and the derivative control eliminates system disturbances. When this type of controller is used in the system, the combination of proportional, integral, and derivative control complements each other, ultimately reducing system errors and bringing them to zero in a short period.

As depicted in Figure 10, the PID controller regulates the platform by continuously adjusting the control signal based on the difference between the desired road input and the measurement obtained from the LPT sensor. In this structure, the control signal is calculated as

$$u(t) = K_p e(t) + K_d \dot{e}(t) + K_i \int e(t)dt \, . \tag{10}$$

Here, the tracking error is defined as $e = x_{1d} - x_1$, where x_{1d} is the desired trajectory and x_1 is the actual position. The three components of the PID controller serve distinct functions: the proportional component, $K_p e(t)$, provides an immediate response to the current error, the integral component, $K_i \int e(t)dt$, eliminates any steady-state error by accumulating past errors, and the derivative component, $K_d \dot{e}(t)$, anticipates future error trends and mitigates them. By combining these components, the PID controller ensures precise control.

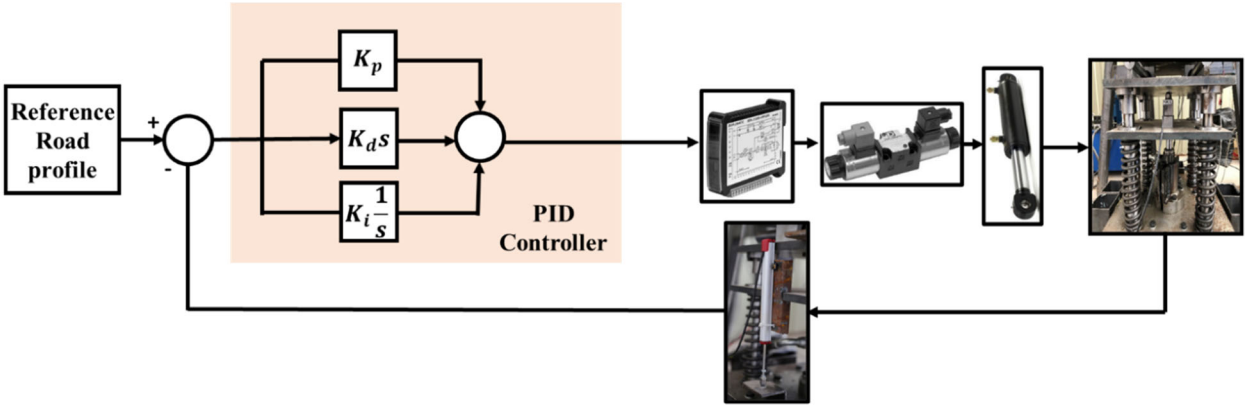

Figure 8. PID control system structure.

5. Results

This section presents the results of implementing the proposed controllers for road input generation. For the fuzzy control, the output conversion gain coefficient is chosen based on the scale of the production outputs, with *Kc*=20. Note that a PCI NI-DAQ-6052 data acquisition card from National Instruments is used for serial communication between the platform and the PC. This card receives sensor signals and transmits control inputs to the system. It has two analog output pins with a bipolar range of -10 to +10 VDC, which we use as control signals in the proposed algorithm. As shown in Figure 7b, the normalized fuzzy control input ranges from -0.4 to 0.4 VDC. To adjust it to the control input range of -8 to +8 VDC, we apply a gain of *Kc*=20 to the fuzzy controller's output. This gain value was carefully selected to avoid saturation within the maximum output capacity of the card. For example, a higher gain would risk exceeding the card's output limits. Finally, the control voltage is linearly converted to the supply voltage of the valve by the DVA.

In the following, a comparison of the proposed fuzzy controller with the conventional PID across various harmonic reference trajectories is presented. In the first scenario, a harmonic reference trajectory with an amplitude of 2 cm is utilized as the reference road input. It is important to note that the gain of the conventional PID is tuned through trial and error to minimize the tracking error. The comparison results, depicted in Figure 9, reveal similar performance between both controllers, with strong tracking ability of the desired trajectory. It is also important to mention that a saturation function is applied to the control voltage input to maintain it within the -8 to 8 volts range. Additionally, Fig. 9d presents the control force generated by the actuator within the ranges of about 200 N to produce the harmonic road inputs.

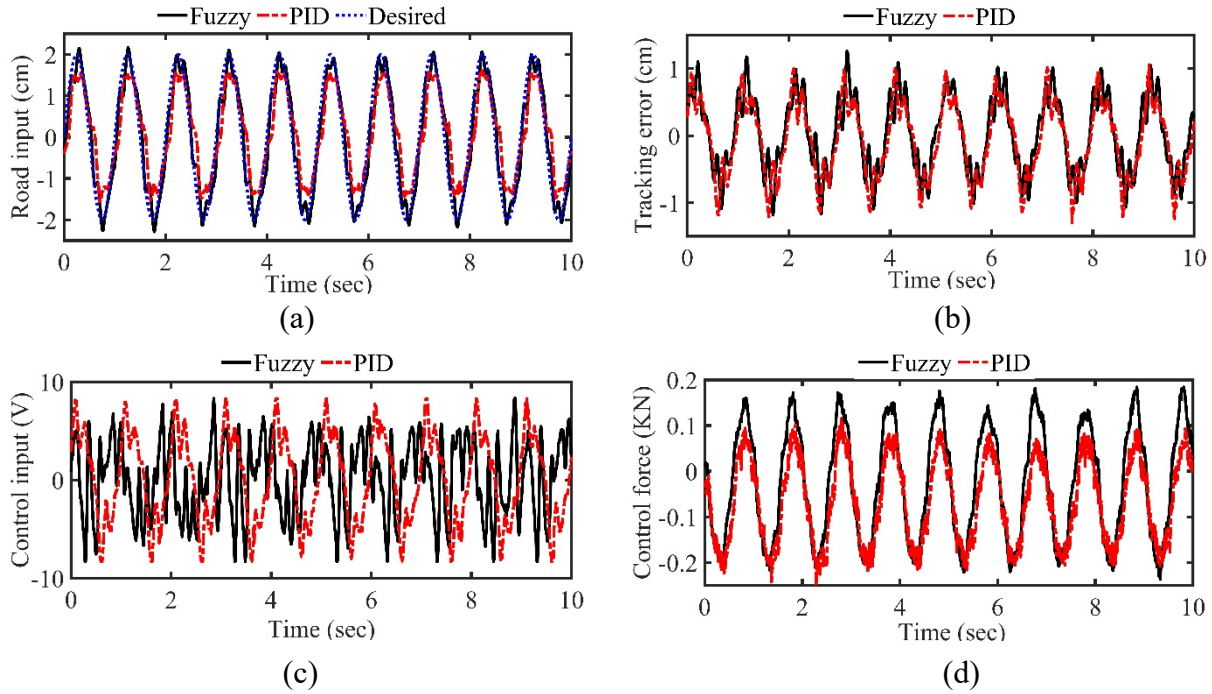

Figure 9. The comparative results of the suggested controller and PID for a harmonic trajectory with the range of 2 cm, (a) Road input, (b) Tracking error, (c) Control input, (d) control force.

To demonstrate the efficiency of the suggested controller on different trajectories, the system's response to a harmonic trajectory with an amplitude of 3 cm is presented in Figure 10. The results from the practical implementation of both controllers for road input generation show that the fuzzy controller exhibits a lower tracking error when following the reference path and generating the road input than the PID controller. This improvement can be attributed to the intelligent nature of the suggested method, which utilizes a soft computing approach for calculating the control input. In contrast, the PID controller attempts to track the reference trajectory using the gains determined in the previous test.

To indicate the independence of the suggested controller from other profiles, the results of both controllers are compared across different periodic trajectories. The comparative results for two periodic trajectories, shown in Figures 11 and 12, highlight the superior efficiency of the suggested fuzzy controller compared to the conventional PID controller. The proposed fuzzy controller can handle nonlinear systems with complex, vague, or imprecise dynamics.

Moreover, the fuzzy control method requires less tuning effort and is more effective when the reference input changes.

To better compare the fuzzy controller and PID in different types of roads, the root mean square (RMS) values of the tracking error are presented in Table 4. The RMS of tracking error for the fuzzy controller is lower than the PID. The comparison results of the fuzzy controller with those obtained by the PID show a reduction between 0.7% and 57% in the RMS of tracking error of the desired road input.

Table 4. Comparison of tracking error RMS in different road-types

Road-Types	RMS of tracking error (cm)		
	Fuzzy	PID	Reduction %
2 cm harmonic	0.5611	0.5653	0.7 %
3 cm harmonic	0.43	1.006	57 %
First periodic	0.3898	0.6430	39 %
Second periodic	0.3034	0.5683	47 %

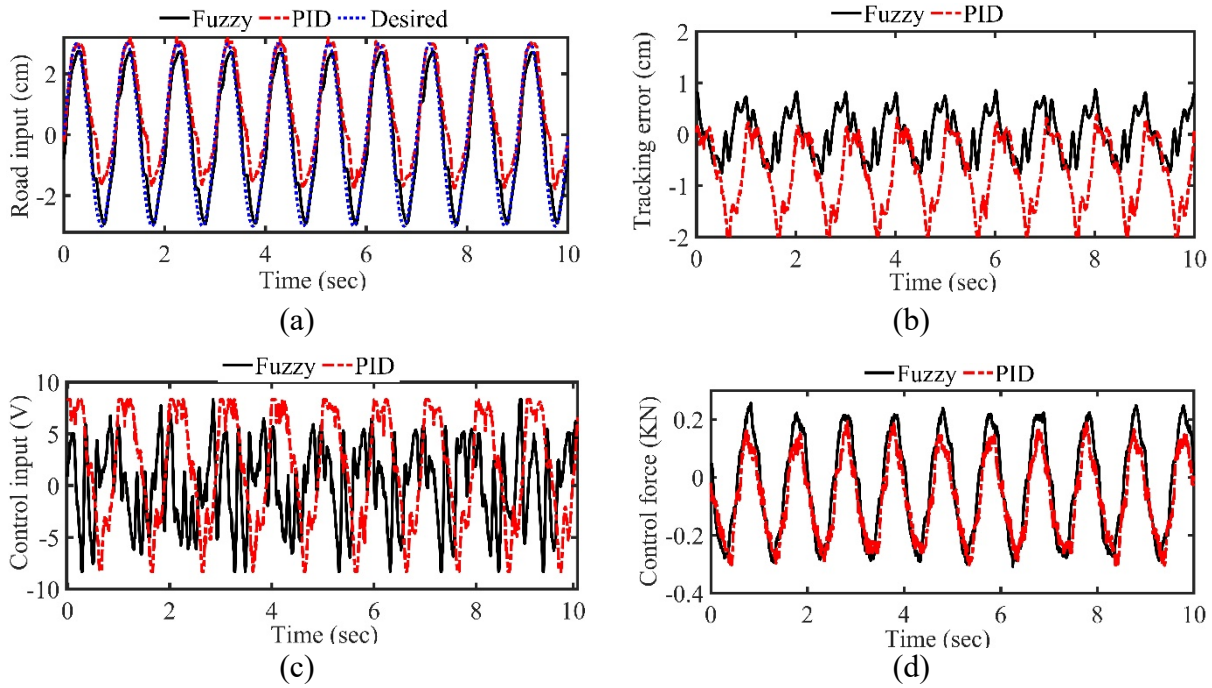

Figure 10. The comparative results of the Fuzzy and PID controllers for a harmonic trajectory with the range of 3 cm, (a) Road input, (b) Tracking error, (c) Control voltage, (d) Control force.#

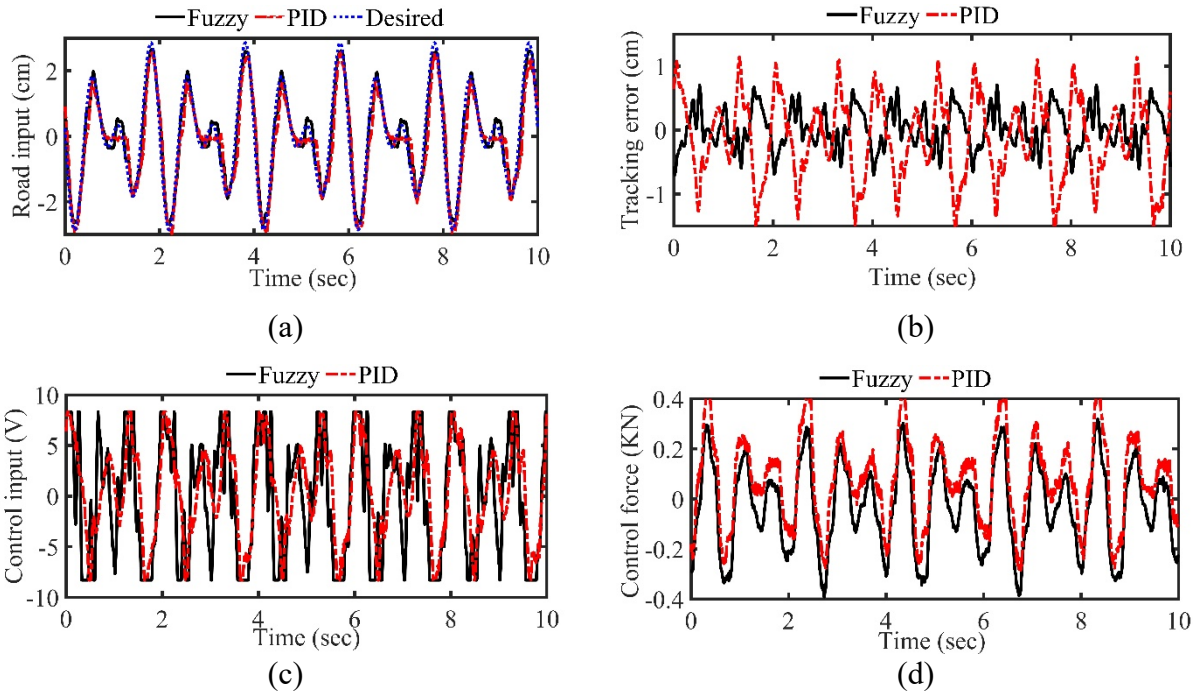

Figure 11. The comparative results of the suggested controller and PID for the first periodic reference road, (a) Road input, (b) Tracking error, (c) Control voltage, (d) Control force.

6. Conclusion

The paper presents the design and experimental evaluation of a fuzzy controller for a road excitation simulator constructed in the laboratory. The fuzzy controller uses Mamdani logic to determine the correct voltage for the electro-hydraulic system based on the displacement data provided by a linear potentiometer transformer. Experimental results from the constructed road simulator platform confirm the effectiveness of the proposed control approach. The findings reveal that the proposed method offers superior accuracy and reliability compared to the conventional PID controller.

(b)

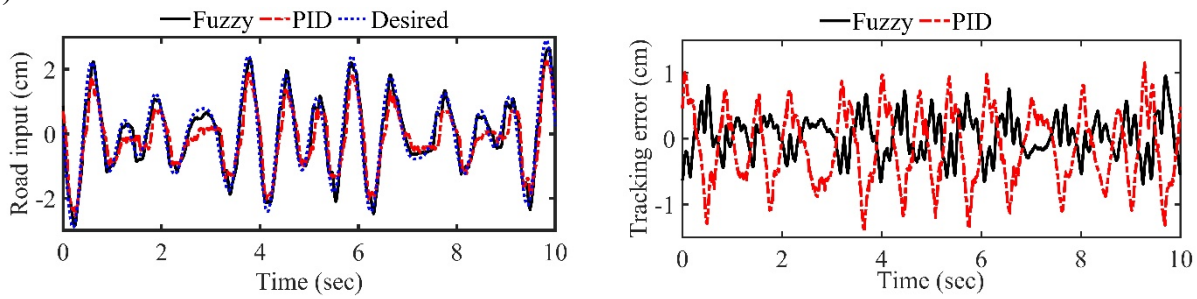

Figure 12. The comparative results of the suggested controller and PID for the second periodic reference road, (a) Road input, (b) Tracking error, (c) Control voltage, (d) Control force.

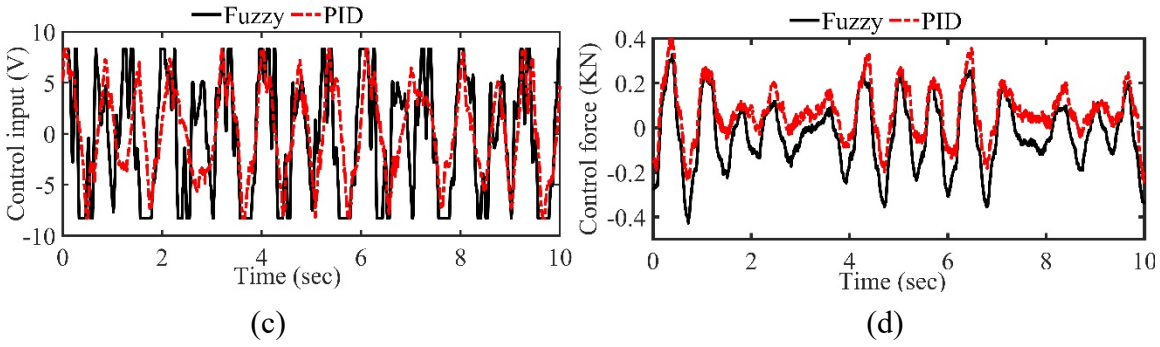

Figure 12. (Cont.) The comparative results of the suggested controller and PID for the second periodic reference road, (a) Road input, (b) Tracking error, (c) Control voltage, (d) Control force.

References

[1] M. Mirzaei, R. Hassannejad, Application of genetic algorithms to optimum design of elasto-damping elements of a half-car model under random road excitations, Proceedings of the Institution of Mechanical Engineers, Part K: Journal of Multi-body Dynamics, 221 (2007) 515-526.

[2] M. Moradi Nerbin, R. Mojed Gharamaleki, M. Mirzaei, Novel optimal control of semi-active suspension considering a hysteresis model for MR damper, Transactions of the Institute of Measurement and Control, 39 (2017) 698-705.

[3] S. Aghasizade, M. Mirzaei, S. Rafatnia, Novel constrained control of active suspension system integrated with anti-lock braking system based on 14-degree of freedom vehicle model, Proceedings of the Institution of Mechanical Engineers, Part K: Journal of Multi-body Dynamics, 232 (2018) 501-520.

[4] A.D. Damavandi, M. Masih-Tehrani, B. Mashadi, Configuration development and optimization of hydraulically interconnected suspension for handling and ride enhancement, Proceedings of the Institution of Mechanical Engineers, Part D: Journal of Automobile Engineering, 236 (2022) 381-394.

[5] H. Gheibollahi, M. Masih-Tehrani, A. Najafi, Improving ride comfort approach by fuzzy and genetic-based PID controller in active seat suspension, International Journal of Automation and Control, 18 (2024) 184-213.

[6] A. Najafi, M. Masih-Tehrani, Lateral safety enhancement in a full dynamic vehicle model based on series active variable-geometry suspension, Journal of Computational Applied Mechanics, 52 (2021) 154-167.

[7] A. Malekshahi, M. Mirzaei, S. Aghasizade, Nonlinear predictive control of multi-input multi-output vehicle suspension system, Journal of Low Frequency Noise, Vibration and Active Control, 34 (2015) 87-105.

[8] R. Azmi, M. Mirzaei, A. Habibzadeh-Sharif, A novel optimal control strategy for regenerative active suspension system to enhance energy harvesting, Energy Conversion and Management, 291 (2023) 117277.

[9] Z.A. Sisi, M. Mirzaei, S. Rafatnia, Estimation of vehicle suspension dynamics with data fusion for correcting measurement errors, Measurement, 231 (2024) 114438.
[10] M.M. Salmani Arani, M. Mirzaei, A. Akbari Alvanagh, S. Aghasizade Shaarbaf, Identification of a nonlinear model for elements of a test rig of quarter car suspension system, Modares Mechanical Engineering, 15 (2016) 136-142.
[11] J. Lin, K.W.E. Cheng, Z. Zhang, N.C. Cheung, X. Xue, Adaptive sliding mode technique-based electromagnetic suspension system with linear switched reluctance actuator, IET Electric Power Applications, 9 (2015) 50-59.
[12] S. Kaka, Pneumatic actuator as vertical dynamic load simulator on the suspension mechanism of a quarter vehicle wheels, ARPN Journal of Engineering and Applied Sciences, 12 (2017) 6975-6980.
[13] G. Koch, E. Pellegrini, S. Spirk, B. Lohmann, Design and modeling of a quarter-vehicle test rig for active suspension control, in, Lehrstuhl für Regelungstechnik, 2010.
[14] A. Akbari, B. Lohmann, Output feedback H∞/GH 2 preview control of active vehicle suspensions: a comparison study of LQG preview, Vehicle System Dynamics, 48 (2010) 1475-1494.
[15] K. Chen, D.G. Beale, Base dynamic parameter estimation of a MacPherson suspension mechanism, Vehicle System Dynamics, 39 (2003) 227-244.
[16] J. Ledwidge, System identification and paramenter estimation of a motorcycle suspension system, in, Dublin City University, 1995.
[17] K. Guo, J. Wei, J. Fang, R. Feng, X. Wang, Position tracking control of electro-hydraulic single-rod actuator based on an extended disturbance observer, Mechatronics, 27 (2015) 47-56.
[18] H.-M. Chen, J.-C. Renn, J.-P. Su, Sliding mode control with varying boundary layers for an electro-hydraulic position servo system, The International Journal of Advanced Manufacturing Technology, 26 (2005) 117-123.
[19] W. Kim, D. Won, D. Shin, C.C. Chung, Output feedback nonlinear control for electro-hydraulic systems, Mechatronics, 22 (2012) 766-777.
[20] M. Tajjudin, N. Ishak, H. Ismail, M.H.F. Rahiman, R. Adnan, Optimized PID control using Nelder-Mead method for electro-hydraulic actuator systems, in: 2011 IEEE Control and System Graduate Research Colloquium, IEEE, 2011, pp. 90-93.
[21] K.M. Elbayomy, J. Zongxia, Z. Huaqing, PID controller optimization by GA and its performances on the electro-hydraulic servo control system, Chinese Journal of Aeronautics, 21 (2008) 378-384.
[22] A. Tony Thomas, R. Parameshwaran, S. Sathiyavathi, A. Vimala Starbino, Improved position tracking performance of electro hydraulic actuator using PID and sliding mode controller, IETE Journal of Research, 68 (2022) 1683-1695.
[23] D.M. Wonohadidjojo, G. Kothapalli, M.Y. Hassan, Position control of electro-hydraulic actuator system using fuzzy logic controller optimized by particle swarm optimization, International Journal of Automation and Computing, 10 (2013) 181-193.
[24] C.-Y. Chen, L.-Q. Liu, C.-C. Cheng, G.T.-C. Chiu, Fuzzy controller design for synchronous motion in a dual-cylinder electro-hydraulic system, Control Engineering Practice, 16 (2008) 658-673.
[25] B. Abdi, M. Mirzaei, S. Rafatnia, A. Akbari Alvanagh, Analytical Design of Constrained Nonlinear Optimal Controller for Vehicle Active Suspension System considering the Limitation of Hydraulic Actuator, Journal of Control, 11 (2017) 25-34.

[26] B. Abdi, M. Mirzaei, R. Mojed Gharamaleki, A new approach to optimal control of nonlinear vehicle suspension system with input constraint, Journal of vibration and control, 24 (2018) 3307-3320.
[27] D. Chindamo, M. Gadola, D. Armellin, F. Marchesin, Design of a road simulator for motorcycle applications, Applied Sciences, 7 (2017) 1220.